THE JOURNAL OF PHYSICAL CHEMISTRY LETTERS
A JOURNAL OF THE AMERICAN CHEMICAL SOCIETY

pubs.acs.org/JPCL

Letter

Suppression of the Phase Coexistence of the fcc–fct Transition in Hafnium-Hydride Thin Films

Lars J. Bannenberg,* Herman Schreuders, Hyunjeong Kim, Kouji Sakaki, Shigenobu Hayashi, Kazutaka Ikeda, Toshiya Otomo, Kohta Asano, and Bernard Dam

Cite This: *J. Phys. Chem. Lett.* 2021, 12, 10969–10974

Read Online

ACCESS | Metrics & More | Article Recommendations | Supporting Information

ABSTRACT: Metal hydrides may play a paramount role in a future hydrogen economy. While most applications are based on nanostructured and confined materials, studies considering the structural response of these materials to hydrogen concentrate on bulk material. Here, using *in situ* in- and out-of-plane X-ray diffraction and reflectometry, we study the fcc ↔ fct transition in Hf thin films, an optical hydrogen-sensing material. We show that the confinement of Hf affects this transition: compared to bulk Hf, the transition is pushed to a higher hydrogen-to-metal ratio, the tetragonality of the fct phase is reduced, and phase coexistence is suppressed. These nanoconfinement effects ensure the hysteresis-free response of hafnium to hydrogen, enabling its remarkable performance as a hydrogen-sensing material. In a wider perspective, the results highlight the profound influences of the nanostructuring and nanoconfinement of metal hydrides on their structural response to hydrogen with a significant impact on their applicability in future devices.

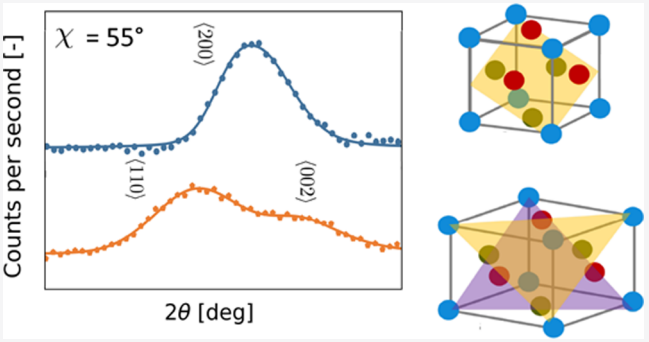

Metal hydrides are a class of materials that may play an important role in a hydrogen-powered economy. Traditionally considered to be hydrogen storage materials,[1−3] other applications such as in hydrogen-purifying membranes,[4,5] switchable mirrors,[6,7] fuel cells,[8] and especially hydrogen sensors[3,9−14] have attracted attention recently. In general, the x (hydrogen-to-metal ratio) − T (temperature) phase diagrams of metal hydrides are relatively complex, involving a combination of body- or face-centered cubic, tetragonal, orthorhombic, or hexagonal metal hydride phases that may or may not coexist.[15] A detailed understanding of (the transitions between) these phases is of vital importance because it determines, together with the entropy and enthalpy of formation, the performance of metal hydrides in real-life applications.

Although many applications of metal hydrides rely on nanostructered materials such as thin films and nanoparticles, most studies determining the phase diagram and nature of phase transitions focused on the bulk. Nanostructuring may significantly alter the properties of metal hydrides, changing their stability and the occurrence of phases and phase transitions (see, e.g., refs 16−24). Such effects may arise from an increased surface-to-volume ratio or, especially for thin films, geometric constraints on the possibility to expand volumetrically and clamping to the supporting substrate. In particular, for hydrogen-sensing applications, metal hydrides are typically structured as thin films or nanoparticles,[3,11−14,25] and understanding the occurrence and nature of phase transitions is of vital importance to designing hysteresis-free hydrogen sensing materials that are stable over time with repeated exposure to hydrogen.

Hafnium (Hf) is a promising optical hydrogen-sensing material that features an extraordinary hysteresis-free sensing range spanning over 6 orders of magnitude in hydrogen pressure.[3,26,27] In the bulk, similar to other group IV elements titanium (Ti)[28−30] and zirconium (Zr),[31,32] a large two-phase region separates the hexagonal-close-packed (hcp) solid solution at low x in HfH_x from the face-centered-cubic (fcc) phase ($x \gtrsim 1.5$), where hydrogen occupies the interstitial tetrahedral sites (4f).[28,33,34] Upon further hydrogenation, a transformation to the face-centered tetragonal (fct) phase is observed, in which the fcc lattice is compressed along the c axis. The attractiveness of hafnium as a hydrogen-sensing material stems from the fact that hafnium thin films show a highly reproducible change in optical transmission in response to a hydrogen exposure ranging over 6 orders of magnitude in hydrogen pressure, which can be used to accurately determine the hydrogen pressure.[3,13,26,27] The sensing range corresponds

Received: October 18, 2021
Accepted: November 1, 2021
Published: November 5, 2021

https://doi.org/10.1021/acs.jpclett.1c03411
J. Phys. Chem. Lett. 2021, 12, 10969−10974

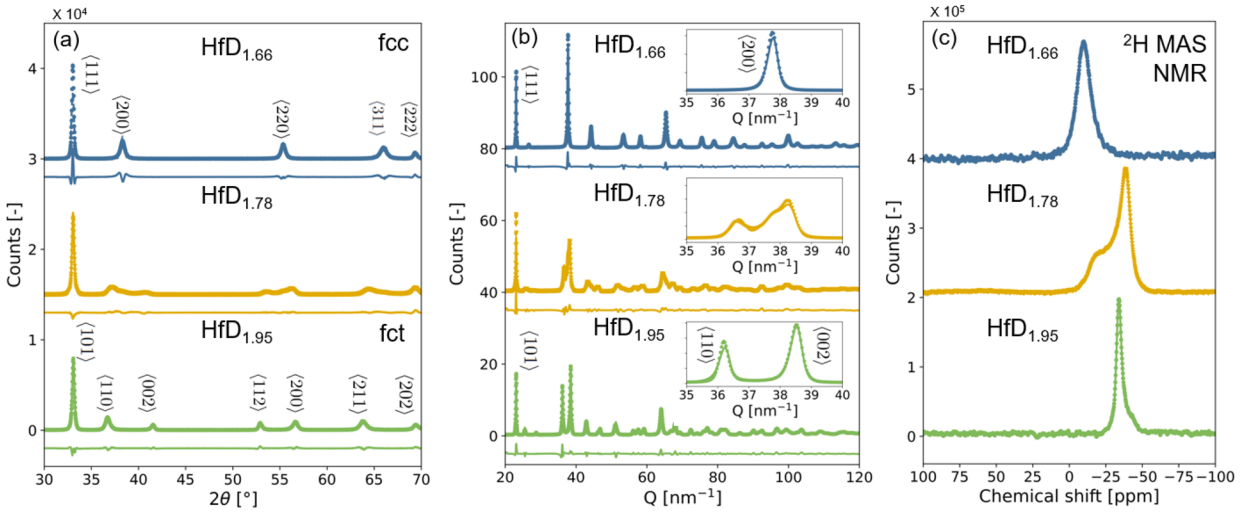

Figure 1. Diffraction and NMR results on powder HfD_x at three different deuteration states: $HfD_{1.66}$, $HfD_{1.78}$, and $HfD_{1.95}$. (a) X-ray diffraction patterns (Cu Kα, λ = 0.1542 nm). The continuous lines show the fit to the data, while the additional lines underneath the diffraction patterns indicate the corresponding residuals of the fits. (b) Neutron diffraction patterns obtained at NOVA located at the Japan Proton Accelerator Research Complex (J-PARC). The insets shows the split of the {200} reflection at $HfD_{1.66}$ to (002) and (110) at $HfD_{1.95}$, while the coexistence of these three reflections is observed at $HfD_{1.78}$. (c) ^{2}H magic angle spinning nuclear magnetic resonance (MAS NMR) spectra.

to a hysteresis-free hydrogenation of Hf from about $HfH_{1.5}$ to $HfH_{1.98}$.[26,27] The appearance of a hysteresis-free sensing range is most remarkable, as for bulk Hf a first-order fcc ↔ fct phase transition involving hysteresis is reported between $HfH_{1.78}$ and $HfH_{1.86}$.[28,34] As such, it is unclear whether the phase transition is suppressed in thin films or whether nanoconfinement pushes the transition toward second order, thereby eliminating the hysteresis. Studying this and other phase transitions in thin films is typically complicated by the strong epi-texturing of the films: while powder X-ray diffraction (XRD) provides information on multiple lattice reflections, typical Bragg–Brentano XRD measurements of thin films provide limited information on the out-of-plane direction only: in the case of hafnium-hydride only the (111) and (222) reflections can be observed, preventing the observation of the fcc ↔ fct phase transition.

Here, we combine *in situ* out-of-plane, in-plane XRD and X-ray reflectometry (XRR) to elucidate the nature of the fcc ↔ fct phase transition in Hf thin films. We unambiguously identify the fcc ↔ fct phase transition in Hf thin films, but at a much larger value of x than in the bulk and with a smaller degree of tetragonality. Different from bulk HfH_x, no sign of phase coexistence is observed, suggesting that the confinement of the film suppresses the phase coexistence. In a more general perspective, these results highlight the profound influence of nanoconfinement on the presence and nature of phase transitions in thin films and other nanostructured metal hydrides.

Before discussing the results on thin films, we first consider the nature of powder Hf to confirm the first-order nature of the fcc ↔ fct phase transition in the bulk. Figure 1 displays X-ray and neutron diffraction results as well as ^{2}H magic angle spinning nuclear magnetic resonance (MAS NMR) spectroscopy results of HfD_x in three different deuteration states—$HfD_{1.66}$, $HfD_{1.78}$, and $HfD_{1.95}$—obtained after pressure–composition isotherm measurements at 300 °C (Figure S3). As previous results indicate that the hafnium–hydrogen and hafnium–deuterium phase diagrams are very similar,[34] we use deuterium instead of hydrogen to suppress the incoherent background in the neutron diffraction experiments and to enable a higher resolution in NMR.

The X-ray and neutron diffraction patterns (Figure 1(a,b)) of $HfD_{1.66}$ and $HfD_{1.95}$ are well described by single-phase models of fcc ($Fm\bar{3}m$) and fct ($I4/mmm$), respectively, while the pattern of $HfD_{1.78}$ can be fitted using only a two-phase model where the fcc and fct phases coexist. While for fitting the XRD pattern the contribution of deuterium is assumed to be negligible, neutron diffraction confirms that deuterium atoms occupy the tetrahedral sites. The lattice parameters that are refined by neutron diffraction are a = 0.487648(6) nm for $HfD_{1.66}$ and a = 0.487805(6) nm and c = 0.434134(10) nm (c/a = 0.89) for $HfD_{1.95}$. The refinement of the pattern for $HfD_{1.78}$ using the two-phase model provides a = 0.467416(33) nm for the fcc phase and a = 0.481491(12) nm and c = 0.443678(26) nm (c/a = 0.92) for the fct phase, respectively. The obtained weight fraction of these two phases is fcc/fct = 39:61.

The ^{2}H MAS NMR spectra confirm the single-phase behavior for $HfD_{1.66}$ and $HfD_{1.95}$ and the phase coexistence for $HfD_{1.78}$. The spectra of $HfD_{1.66}$ and $HfD_{1.95}$ show a single component (Figure 1(c)), which have negative Knight shifts of −9.9 and −33.9 ppm, respectively. The Knight shift is attributed to the density of states at the Fermi energy: $HfD_{1.66}$ is relatively more insulating than $HfD_{1.95}$, consistent with the reduction of the optical transmission upon increased hydrogenation (Figure 4(d,e) and refs 26 and 27). The spectrum of $HfD_{1.78}$ consists of two contributions due to the phase coexistence. As such, it was fitted using two Gaussian functions with an area ratio of fcc/fct = 4:6. Assuming that the deuterium contents of the fcc and fct phases are D/Hf = 1.75 and 2, respectively, and using the fact that the intensity of NMR signals is proportional to the molar ratio of deuterium, the weight fraction is estimated to be fcc/fct = 43:57, which is close to the one obtained by neutron diffraction. Most importantly, the phase coexistence observed for $HfD_{1.78}$ by both X-ray and neutron diffraction as well as NMR unambiguously confirms the first-order nature of the fcc–fct phase transition.

https://doi.org/10.1021/acs.jpclett.1c03411
J. Phys. Chem. Lett. 2021, 12, 10969−10974

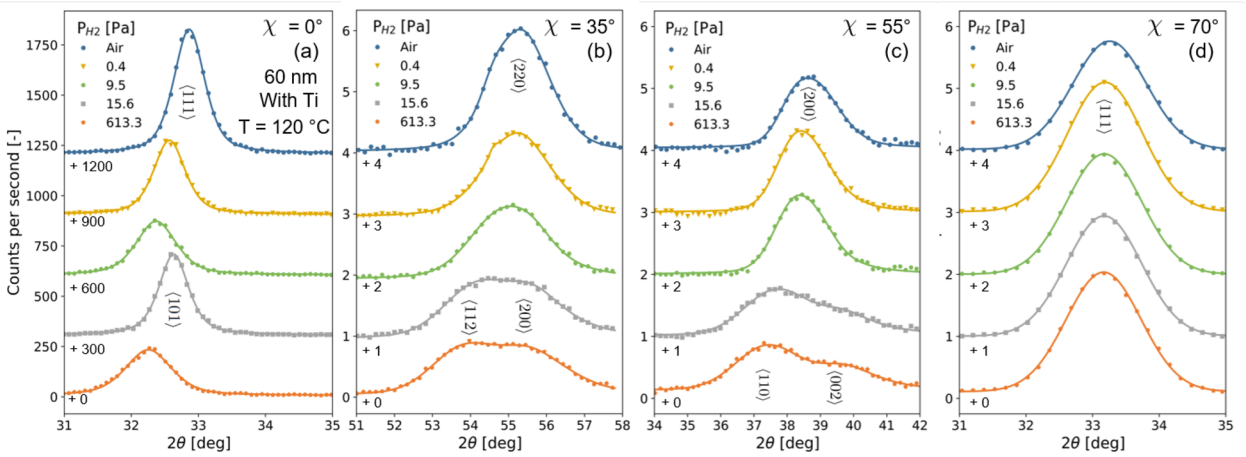

Figure 2. *In situ* out-of-plane and in-plane XRD measurements (Cu Kα, λ = 0.1542 nm) on the 60 nm Hf films capped with a 10 nm Pd layer and with a 3 nm Ti adhesion layer at T = 120 °C and the partial hydrogen pressures P_{H_2} indicated. During the experiment, the hydrogen pressure was increased stepwise. (a) Out-of-plane diffraction and in-plane diffraction with the sample tilted in the direction perpendicular to the X-ray beam by (b) χ = 35°, (c) χ = 55°, and (d) χ = 70°. The continuous lines show fits of pseudo-Voigt function(s) to the data from which the d spacing (Figure 3) has been derived.

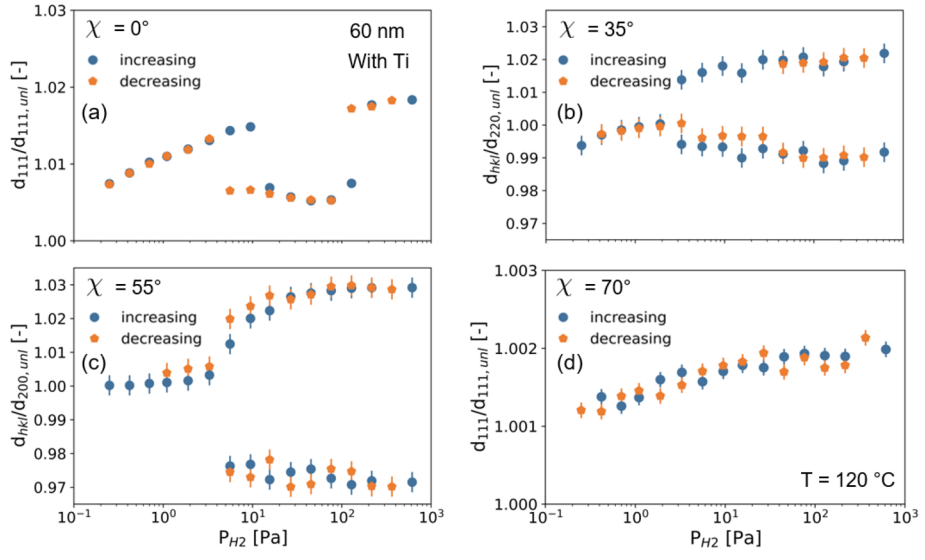

Figure 3. Partial hydrogen pressure dependence of the *in situ* out-of-plane and in-plane d spacing of 60 nm Hf films capped with a 10 nm Pd layer and with a 3 nm Ti adhesion layer at T = 120 °C. During the experiment, the hydrogen pressure was stepwise increased and decreased. The d spacing was obtained by fitting pseudo-Voigt functions to the data of Figure 2 and normalized to the d spacing of the unloaded state as measured in air. d spacing was obtained by (a) out-of-plane diffraction and in-plane diffraction with the sample tilted in the direction perpendicular to the X-ray beam by (b) χ = 35°, (c) χ = 55°, and (d) χ = 70°.

Turning to the results of the thin films, Figure 2 displays the out-of-plane and in-plane diffraction measurements obtained for different partial hydrogen pressures at 120 °C. The thin films are produced by magnetron sputtering on fused quartz substrates and are composed of a 4 nm Ti adhesion, a 60 nm Hf, and a 10 nm Pd capping layer to prevent oxidation and promote hydrogen dissociation. As the films are highly textured, the out-of-plane results reveal only the (111) peak (Figures S4 Figure S5). As such, we performed in-plane diffraction by tilting the sample in the direction perpendicular to the beam by ϕ = 35, 55, and 70° in order to monitor the hydrogen pressure dependence of the (200), (220), and in-plane (111) reflections.

Most importantly, the diffraction patterns show the hallmarks of the fcc ↔ fct transformation: comparing the diffraction patterns in the unloaded state and the highest hydrogen pressure measured, P_{H_2} = 613 Pa, indicates that the (111) reflection (Figure 2(a,d)) remains unsplit, both in the in- and out-of-plane directions, while the (200) (Figure 2(b)) and (220) (Figure 2(c)) reflections, both oriented in-plane, each split into two peaks. On the basis of the peak positions, we observe a substantial expansion of the a axes from 0.472 nm in the unloaded state to 0.479 nm in the fully hydrated state. At the same time, the c axis contracts to 0.457 nm, resulting in $c/a \approx 0.95$. As such, the volume of the unit cell in the fully hydrogenated state of V = 0.0524 nm^3 is approximately the same as for the bulk (V = 0.0516 nm^3), while the compression of the c axis and expansion of the a axes are much less pronounced in the thin films than in the bulk ($c/a \approx 0.90$).

https://doi.org/10.1021/acs.jpclett.1c03411
J. Phys. Chem. Lett. 2021, 12, 10969−10974

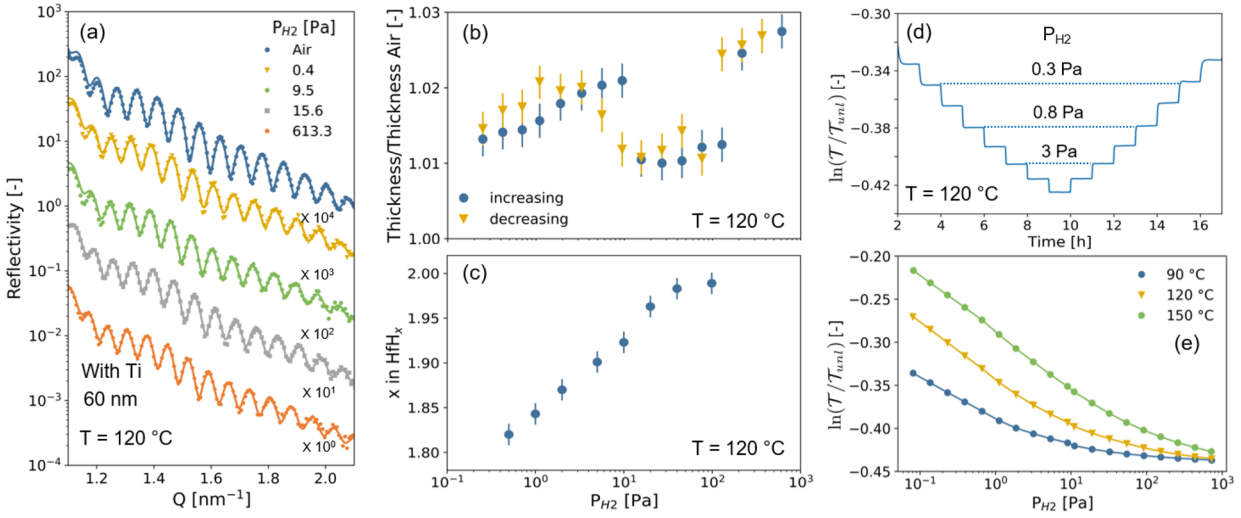

Figure 4. Reflectometry and optical transmission measurements on the 60 nm Hf films capped with a 10 nm Pd layer and with a 3 nm Ti adhesion layer. (a) *In situ* X-ray reflectometry (XRR) measurements at T = 120 °C and the partial hydrogen pressures P_{H_2} indicated. During the experiment, the hydrogen pressure was stepwise increased. The dots indicate the measurement points, while the continuous lines indicate the fits to the data. (b) Partial hydrogen pressure dependence of the Hf layer thickness at T = 120 °C derived from fitting the XRR data that was collected by stepwise increasing and decreasing the partial hydrogen pressure. (c) Hydrogen content at T = 120 °C of 40 nm Hf films capped with a 10 nm Pd layer as deduced from neutron reflectometry measurements. Data were obtained from ref 27. (d) Changes in the white light optical transmission where the film was exposed to various increasing and decreasing pressure steps of P_{H_2} = 0.22−9.5 Pa at T = 120 °C. The optical transmission $\mathcal{T}$ is measured relative to the transmission of the film after unloading in air ($\mathcal{T}_{unl}$). The dashed lines indicate levels of the same transmission and pressure. (e) Partial hydrogen pressure dependence of changes in the white light optical transmission at T = 90, 120, and 150 °C.

The fcc ↔ fct transition at $P_{H_2} = 10^{+1}$ Pa is accompanied by a considerable reduction in volume. The out-of-plane diffraction results indicate a reduction of the out-of-plane d_{111} spacing by about 1% (Figure 3(a)) when fcc ↔ fct occurs. Differently, the in-plane d_{111} spacing remains unaltered and thus does not change upon increased hydrogenation. Consistent with this, the XRR measurements of Figure 4(a,b) indicate that the Hf layer thickness decreases by about 1%, thus indicating that the reduction of the d_{111} spacing is translated completely in the out-of-plane direction.

Different from bulk measurements, where phase coexistence of fcc- and fct-HfH$_x$ is observed in the region between $x \approx 1.78$ and $x \approx 1.86$,[34] the XRD patterns of thin film Hf do not show any indication of the simultaneous occurrence of these two phases. The absence of phase coexistence in thin films could imply that the confinement of the film suppresses the phase coexistence associated with a first order phase transition. It has the important implication that the hysteresis associated with first-order phase transition is (practically) eliminated. Indeed, both earlier[26,27] and present (Figure 4(d,e)) optical transmission measurements of Hf indicate a completely hysteresis-free response to changing hydrogen pressures: The optical transmission at a certain P_{H_2} is exactly the same after increasing and decreasing the pressure, making the response of hafnium as an optical sensing material completely free of hysteresis.

In addition, we observe that the phase transition in thin films occurs at a much larger x than in the bulk. Both our data (Figure 1) and data in the literature (see, e.g., refs 28 and 34) indicate that the onset of the transition occurs at $x \approx 1.78$ in the bulk. For thin films, neutron reflectometry measurements (Figure 4(c)) indicate that the partial pressure of the transition, $P_{H_2} \approx 10$ Pa, corresponds to $x \approx 1.92$. Different from bulk materials, two-dimensional films that are clamped to the substrate have to obey constraints on lateral expansion because expansion can be realized only in the out-of-plane direction, which may result in a very high in-plane stress and affect the stability of phases.[17,22,23,35,36] Indeed, the diffraction results indicate that the unit cell expands only in the out-of-plane direction and continuously deforms from its unloaded state: at P_{H_2} = 9.5 Pa (HfH$_{1.90}$), the out-of-plane d_{111} spacing is approximately 2% longer than the in-plane spacing (Figure 2(a,d)). Moreover, the nucleation of domains, inducing locally large stresses, may also be hindered considerably by the clamping of the film to the substrate.[22,24,35,37−40] The collective result of the clamping is that the onset of the transition is pushed to higher values of x, the coexistence of phases is suppressed, and the tetragonality is much smaller than for the bulk.

Most remarkable is that an abrupt increase in both the out-of-plane d_{111} spacing (Figure 3(a)) and layer thickness (Figure 4(b)) of about 1% is observed at $P_{H_2} = 10^{+2}$ Pa, while no changes are seen in the in-plane XRD results. Neutron reflectometry measurements (Figure 4(c)) reproduced from ref 27 indicate that this abrupt change in layer thickness and d_{111} spacing occurs when the layer is nearly fully hydrogenated, i.e., at $x \approx 1.98$. While we have no direct explanation for this remarkable observation, a direction for future research would be to determine if such a volume reduction also occurs in other group IV elements Zr and Ti.

In the literature, the root cause of changes in the optical transmission of metal hydride thin films upon exposure to hydrogen has been debated. Often, Beer-Lambert's law is taken as a staring point: $T = I/I(d) = e^{-\alpha d}$, with T the optical transmission of the film, d the thickness and α the linear attanuation coefficient. In this framework, changes in the optical transmission upon hydrogenation can be due to the volumetric expansion of the film (that needs to be completely translated in an expansion of the film thickness d) or to

https://doi.org/10.1021/acs.jpclett.1c03411
J. Phys. Chem. Lett. 2021, 12, 10969−10974

differences in hydrogen concentration in the metallic thin film causing changes to the dielectric constants and thus the adsorption coeficient α. Different from a previous study of vanadium films for which it was reported that the optical transmission changes are driven by the volumetric expansion of the thin film,[41] our results are consistent with optical transmission changes dictated by changes in the hydrogen concentration affecting the dielectric properties. Indeed, the fcc ↔ fct transition including the pronounced reduction in volume is not reflected in the partial pressure dependence of the optical transmission that changes monotonically with increasing partial hydrogen pressure (Figure 4(d,e)). Thus, our results suggests that the changes in optical transmission are fully dictated by the change in hydrogen concentration, causing changes to the dielectric properties, and not by the variation of the thickness of the thin film. This is consistent with neutron reflectometry and optical transmission measurements of Hf[26] (and Ta,[27] $Pd_{1-y}Au_y$[24]) that indicate a linear relationship between the optical transmission and the hydrogen concentration of the metallic layer. The fact that the optical transmission is unaffected by the fcc ↔ fct transition has the convenient implication that Hf can be used as a hydrogen sensor in which the optical response monotonically changes with the hydrogen pressure/concentration in the environment over a large range.

In conclusion, using *in situ* in- and out-of-plane X-ray diffraction and reflectometry, we unambiguously identify that the fcc ↔ fct transition also exists in Hf thin films. The confinement of Hf and the clamping to the substrate significantly affect the transition: compared to bulk Hf, the transition is pushed to higher values of x, the tetragonality of the fct phase is reduced, and the coexistence of phases is suppressed. These results highlight the profound influences of the nanoconfinement of metal hydrides on their structural response to hydrogen. In the case of Hf, the nanoconfinement effects facilitate the extraordinary performance as an optical hydrogen-sensing material including a hysteresis-free sensing range over 6 orders of magnitude in partial hydrogen pressure.

■ ASSOCIATED CONTENT

Supporting Information

The Supporting Information is available free of charge at https://pubs.acs.org/doi/10.1021/acs.jpclett.1c03411.

Experimental details; spectrum of the LED lights used for the optical transmission measurements; photographs of the *in situ* XRD/XRR setup. Pressure−composition isotherm of bulk powder HfD_x; out-of-plane and in-plane XRD measurements of the Hf thin films; and rocking curves of the Hf thin films (PDF)

■ AUTHOR INFORMATION

Corresponding Author

Lars J. Bannenberg − *Faculty of Applied Sciences, Delft University of Technology, 2629 JB Delft, The Netherlands;* orcid.org/0000-0001-8150-3694; Email: l.j.bannenberg@tudelft.nl

Authors

Herman Schreuders − *Faculty of Applied Sciences, Delft University of Technology, 2629 JB Delft, The Netherlands*

Hyunjeong Kim − *Energy Process Research Institute, National Institute of Advanced Industrial Science and Technology (AIST), Tsukuba, Ibaraki 305-8569, Japan;* orcid.org/0000-0001-5018-3173

Kouji Sakaki − *Energy Process Research Institute, National Institute of Advanced Industrial Science and Technology (AIST), Tsukuba, Ibaraki 305-8569, Japan;* orcid.org/0000-0003-4781-1073

Shigenobu Hayashi − *Research Institute for Material and Chemical Measurement, National Institute of Advanced Industrial Science and Technology (AIST), Tsukuba, Ibaraki 305-8565, Japan;* orcid.org/0000-0001-9085-6600

Kazutaka Ikeda − *Institute of Materials Structure Science, High Energy Accelerator Research Organization (KEK), Tokai 319-1106, Japan*

Toshiya Otomo − *Institute of Materials Structure Science, High Energy Accelerator Research Organization (KEK), Tokai 319-1106, Japan*

Kohta Asano − *Energy Process Research Institute, National Institute of Advanced Industrial Science and Technology (AIST), Tsukuba, Ibaraki 305-8569, Japan;* orcid.org/0000-0003-4208-7303

Bernard Dam − *Faculty of Applied Sciences, Delft University of Technology, 2629 JB Delft, The Netherlands;* orcid.org/0000-0002-8584-7336

Complete contact information is available at: https://pubs.acs.org/10.1021/acs.jpclett.1c03411

Notes

The authors declare no competing financial interest.

■ ACKNOWLEDGMENTS

We thank Malte Verleg for designing the sample holders for the in-plane *in situ* XRD measurements, Martin Exeter for fabricating these sample holders from Al, Joost Middelkoop for 3D printing the sample holders, and Reinier den Oudsten for making a spacer for the Anton Paar XRK900 reactor chamber such that the tilted *in situ* measurements could be performed at the correct height. Quan van der Knokke is acknowledged for fruitful discussions. The neutron scattering experiments were approved by the Neutron Scattering Program Advisory Committee of the Institute of Materials Structure Science (IMSS), High Energy Accelerator Research Organization (KEK) (proposal no. 2014S06).

■ REFERENCES

(1) Rusman, N. A. A.; Dahari, M. A Review on the Current Progress of Metal Hydrides Material for Solid-State Hydrogen Storage Applications. *Int. J. Hydrogen Energy* **2016**, *41*, 12108−12126.

(2) Schneemann, A.; White, J. L.; Kang, S.; Jeong, S.; Wan, L. F.; Cho, E. S.; Heo, T. W.; Prendergast, D.; Urban, J. J.; Wood, B. C.; et al. Nanostructured Metal Hydrides for Hydrogen Storage. *Chem. Rev.* **2018**, *118*, 10775−10839.

(3) Bannenberg, L. J.; Heere, M.; Benzidi, H.; Montero, J.; Dematteis, E.; Suwarno, S.; Jaron, T.; Winny, M.; OrÅĆowski, P.; Wegner, W.; et al. Metal (boro-) Hydrides for High Energy Density Storage and Relevant Emerging Technologies. *Int. J. Hydrogen Energy* **2020**, *45*, 33687−33730.

(4) Nishimura, C.; Komaki, M.; Hwang, S.; Amano, M. V. −Ni Alloy Membranes for Hydrogen Purification. *J. Alloys Compd.* **2002**, *330*, 902−906.

(5) Dolan, M. D.; Viano, D. M.; Langley, M. J.; Lamb, K. E. Tubular Vanadium Membranes for Hydrogen Purification. *J. Membr. Sci.* **2018**, *549*, 306−311.

(6) Huiberts, J. N.; Griessen, R.; Rector, J. H.; Wijngaarden, R. J.; Dekker, J. P.; De Groot, D. G.; Koeman, N. J. Yttrium and

Lanthanum Hydride Films with Switchable Optical Properties. *Nature* **1996**, *380*, 231−234.
(7) Maiorov, V. A. Metal Hydride Switchable Mirrors. *Opt. Spectrosc.* **2020**, *128*, 148−165.
(8) Lototskyy, M. V.; Tolj, I.; Pickering, L.; Sita, C.; Barbir, F.; Yartys, V. The Use of Metal Hydrides in Fuel Cell Applications. *Prog. Nat. Sci.* **2017**, *27*, 3−20.
(9) Hübert, T.; Boon-Brett, L.; Black, G.; Banach, U. Hydrogen Sensors−a Review. *Sens. Actuators, B* **2011**, *157*, 329−352.
(10) Wadell, C.; Syrenova, S.; Langhammer, C. Plasmonic hydrogen sensing with nanostructured metal hydrides. *ACS Nano* **2014**, *8*, 11925−11940.
(11) Bannenberg, L. J.; Boelsma, C.; Asano, K.; Schreuders, H.; Dam, B. Metal Hydride Based Optical Hydrogen Sensors. *J. Phys. Soc. Jpn.* **2020**, *89*, 051003.
(12) Darmadi, I.; Nugroho, F. A. A.; Langhammer, C. High-Performance Nanostructured Palladium-Based Hydrogen Sensors−Current Limitations and Strategies for Their Mitigation. *ACS Sensors* **2020**, *5*, 3306−3327.
(13) Koo, W.-T.; Cho, H.-J.; Kim, D.-H.; Kim, Y. H.; Shin, H.; Penner, R. M.; Kim, I.-D. Chemiresistive Hydrogen Sensors: Fundamentals, Recent Advances, and Challenges. *ACS Nano* **2020**, *14*, 14284−14322.
(14) Chen, K.; Yuan, D.; Zhao, Y. Review of Optical Hydrogen Sensors Based on Metal Hydrides: Recent Developments and Challenges. *Opt. Laser Technol.* **2021**, *137*, 106808.
(15) Manchester, F. D. *Phase Diagrams of Binary Hydrogen Alloys*; ASM International, 2000.
(16) Feenstra, R.; de Bruin-Hordijk, G. J.; Bakker, H. L. M.; Griessen, R.; de Groot, D. G. Critical Point Lowering in Thin PdH_x Films. *J. Phys. F: Met. Phys.* **1983**, *13*, L13.
(17) Pivak, Y.; Gremaud, R.; Gross, K.; Gonzalez-Silveira, M.; Walton, A.; Book, D.; Schreuders, H.; Dam, B.; Griessen, R. Effect of the Substrate on the Thermodynamic Properties of PdH_x Films Studied by Hydrogenography. *Scr. Mater.* **2009**, *60*, 348−351.
(18) Bloch, J.; Pejova, B.; Jacob, J.; Hjörvarsson, B. Hydrogen-Vanadium System in Thin Films: Effect of Film Thickness. *Phys. Rev. B: Condens. Matter Mater. Phys.* **2010**, *82*, 245428.
(19) Baldi, A.; Narayan, T. C.; Koh, A. L.; Dionne, J. A. In situ Detection of Hydrogen-Induced Phase Transitions in Individual Palladium Nanocrystals. *Nat. Mater.* **2014**, *13*, 1143−1148.
(20) Syrenova, S.; Wadell, C.; Nugroho, F. A. A.; Gschneidtner, T. A.; Fernandez, Y. A. D.; Nalin, G.; Świtlik, D.; Westerlund, F.; Antosiewicz, T. J.; Zhdanov, V. P.; et al. Hydride Formation Thermodynamics and Hysteresis in Individual Pd Nanocrystals with Different Size and Shape. *Nat. Mater.* **2015**, *14*, 1236−1244.
(21) Griessen, R.; Strohfeldt, N.; Giessen, H. Thermodynamics of the Hybrid Interaction of Hydrogen with Palladium Nanoparticles. *Nat. Mater.* **2016**, *15*, 311−317.
(22) Burlaka, V.; Wagner, S.; Hamm, M.; Pundt, A. Suppression of Phase Transformation in Nb−H Thin Films below Switchover Thickness. *Nano Lett.* **2016**, *16*, 6207−6212.
(23) Wagner, S.; Pundt, A. Quasi-Thermodynamic Model on Hydride Formation in Palladium−Hydrogen Thin Films: Impact of Elastic and Microstructural Constraints. *Int. J. Hydrogen Energy* **2016**, *41*, 2727−2738.
(24) Bannenberg, L. J.; Nugroho, F. A. A.; Schreuders, H.; Norder, B.; Trinh, T. T.; Steinke, N.-J.; Van Well, A. A.; Langhammer, C.; Dam, B. Direct Comparison of PdAu Alloy Thin Films and Nanoparticles upon Hydrogen Exposure. *ACS Appl. Mater. Interfaces* **2019**, *11*, 15489−15497.
(25) Bannenberg, L. J.; Boshuizen, B.; Ardy Nugroho, F. A.; Schreuders, H. Hydrogenation kinetics of metal hydride catalytic layers. *ACS Appl. Mater. Interfaces* **2021**, DOI: 10.1021/acsami.1c13240.
(26) Boelsma, C.; Bannenberg, L. J.; van Setten, M. J.; Steinke, N.-J.; Van Well, A. A.; Dam, B. Hafnium - an Optical Hydrogen Sensor Spanning Six Orders in Pressure. *Nat. Commun.* **2017**, *8*, 15718.
(27) Bannenberg, L. J.; Boelsma, C.; Schreuders, H.; Francke, S.; Steinke, N.-J.; Van Well, A. A.; Dam, B. Optical Hydrogen Sensing Beyond Palladium: Hafnium and Tantalum as Effective Sensing Materials. *Sens. Actuators, B* **2019**, *283*, 538−548.
(28) Sidhu, S. S.; Heaton, L.; Zauberis, D. D. Neutron Diffraction Studies of Hafnium−Hydrogen and Titanium−Hydrogen Systems. *Acta Crystallogr.* **1956**, *9*, 607−614.
(29) San-Martin, A.; Manchester, F. D. The H-Ti (hydrogen-titanium) system. *Bull. Alloy Phase Diagrams* **1987**, *8*, 30−42.
(30) Lewkowicz, I. Titanium-Hydrogen. *Solid State Phenomena* **1996**, *49-50*, 239−280.
(31) Zuzek, E.; Abriata, J. P.; San-Martin, A.; Manchester, F. D. The H-Zr (Hydrogen-Zirconium) System. *Bull. Alloy Phase Diagrams* **1990**, *11*, 385−395.
(32) Aladjem, A. Zirconium-Hydrogen. *Solid State Phenomena* **1996**, *49-50*, 281−330.
(33) Sidhu, S. S.; McGuire, J. C. An X-ray Diffraction Study of the Hafnium-Hydrogen System. *J. Appl. Phys.* **1952**, *23*, 1257−1261.
(34) Mintz, M. H. Hafnium-Hydrogen. *Solid State Phenomena* **1996**, *49-50*, 331−356.
(35) Pundt, A.; Kirchheim, R. Hydrogen in Metals: Microstructural Aspects. *Annu. Rev. Mater. Res.* **2006**, *36*, 555−608.
(36) Wagner, S.; Pundt, A. Mechanical Stress Impact on Thin $Pd_{1-x}Fe_x$ Film Thermodynamic Properties. *Appl. Phys. Lett.* **2008**, *92*, 051914.
(37) Mooij, L.; Dam, B. Hysteresis and the Role of Nucleation and Growth in the Hydrogenation of Mg Nanolayers. *Phys. Chem. Chem. Phys.* **2013**, *15*, 2782−2792.
(38) Bannenberg, L. J.; Schreuders, H.; van Eijck, L.; Heringa, J. R.; Steinke, N.-J.; Dalgliesh, R.; Dam, B.; Mulder, F. M.; van Well, A. A. Impact of Nanostructuring on the Phase Behavior of Insertion Materials: The Hydrogenation Kinetics of a Magnesium Thin Film. *J. Phys. Chem. C* **2016**, *120*, 10185−10191.
(39) Baldi, A.; Mooij, L.; Palmisano, V.; Schreuders, H.; Krishnan, G.; Kooi, B. J.; Dam, B.; Griessen, R. Elastic versus Alloying Effects in Mg-Based Hydride Films. *Phys. Rev. Lett.* **2018**, *121*, 255503.
(40) Wagner, S.; Klose, P.; Burlaka, V.; Nörthemann, K.; Hamm, M.; Pundt, A. Structural Phase Transitions in Niobium Hydrogen Thin Films: Mechanical Stress, Phase Equilibria and Critical Temperatures. *ChemPhysChem* **2019**, *20*, 1890−1904.
(41) Droulias, S.; Granas, O.; Hartmann, O.; Komander, K.; Hjorvarsson, B.; Wolff, M.; Palsson, G. The Root Cause of Hydrogen Induced Changes in Optical Transmission of Vanadium. *arXiv:1812.04917*, **2018**.

https://doi.org/10.1021/acs.jpclett.1c03411
J. Phys. Chem. Lett. 2021, 12, 10969−10974